

Border collision bifurcations in a two-dimensional piecewise smooth map from a simple switching circuit

Laura Gardini,^{1,a)} Danièle Fournier-Prunaret,^{2,b)} and Pascal Chargé^{2,c)}

¹*Department of Economics, Society and Politics, University of Urbino, 61029 Urbino, Italy*

²*LATTIS-INSA, Université de Toulouse, France*

(Received 1 November 2010; accepted 14 January 2011; published online 13 April 2011)

In recent years, the study of chaotic and complex phenomena in electronic circuits has been widely developed due to the increasing number of applications. In these studies, associated with the use of chaotic sequences, chaos is required to be robust (not occurring only in a set of zero measure and persistent to perturbations of the system). These properties are not easy to be proved, and numerical simulations are often used. In this work, we consider a simple electronic switching circuit, proposed as chaos generator. The object of our study is to determine the ranges of the parameters at which the dynamics are chaotic, rigorously proving that chaos is robust. This is obtained showing that the model can be studied via a two-dimensional piecewise smooth map in triangular form and associated with a one-dimensional piecewise linear map. The bifurcations in the parameter space are determined analytically. These are the border collision bifurcation curves, the degenerate flip bifurcations, which only are allowed to occur to destabilize the stable cycles, and the homoclinic bifurcations occurring in cyclical chaotic regions leading to chaos in 1-piece.

© 2011 American Institute of Physics. [doi:10.1063/1.3555834]

The study of chaotic systems, either to control or to be used in chaotic regimes, is nowadays of wide interest. These studies are often associated with the analysis of switching systems, leading to piecewise smooth models, either in continuous or in discrete time. An important result, often difficult to get, is the analysis of the regimes in which stable dynamics or chaotic dynamics occur. Sometimes, the results are based on numerical evidence, which, however, may be not reliable. In the present work, we propose a switching circuit as chaos generator. This system is both simple to construct and chaotic. We can give a rigorous proof of the chaotic behavior, which occurs in wide regions and is robust: it occurs in a set of positive measure and is persistent under parameter variations. A peculiarity of the proposed system is that, due to an intrinsic symmetry, it can be either studied via a one-dimensional (1D) skew-tent map or via a two-dimensional piecewise smooth map in triangular form, which has a driving function also strictly related with a one-dimensional skew-tent map. This allows us to prove our results, showing that the flip bifurcations of cycles are all degenerated, which means that the flip bifurcations are not leading to a cycle of double period close to the bifurcating one. We prove that the appearance/disappearance of k -cycles is due to border collision bifurcations. All the bifurcations are analytically detected, leading to a complete description of the periodicity regions in the parameters space, as well as of the regions associated with robust chaotic sets.

I. INTRODUCTION

In the last two decades, a wide interest in the studies of chaotic and complex phenomena in electronic circuits and systems has been observed. These studies are associated with the increasing number of applications that successfully utilize chaotic sequences. Chaos generators are used in several context: secure communications, noise radar and sonar, signal processing, industrial electronics, as well as for other purposes (see Refs. 1–5, to cite a few). Otherwise, vice versa studies are performed in order to avoid chaotic regimes (as in chaos control theory^{6–8}). In both cases, the object is the knowledge of the parameter regions in which chaos occurs.

Moreover, in the case of chaos generators, it is also important that the generator is easy and simple to construct and to be sure that the regime is really chaotic, occurring in a wide set not due to a numerical effect, and such that a small perturbation cannot lead to the disappearance of the chaotic sequence. This motivates the present work in the study of new chaotic systems. The model here proposed satisfies both the objectives. It is obtained via a simple switching circuit, and we fully describe the dynamic behaviors, showing precisely the regions with attracting periodic orbits, as well as the wide regions of robust chaos (i.e., persistent, or structurally stable, and occurring in a set of positive measure, see also Ref. 9).

The use of a switching system is quite common nowadays. In fact, several applied models are described by switching system, due to their applicability in a large number of practical systems, not only in electronics. Many examples are shown in the survey books.^{10–12} These systems are described by piecewise smooth functions, either in continuous or in discrete time, and the study of their dynamics leads to a new kind of bifurcations, due to the switching manifolds.

^{a)}Electronic mail: laura.gardini@uniurb.it.

^{b)}Electronic mail: danièle.fournier@insa-toulouse.fr.

^{c)}Electronic mail: pascal.charge@insa-toulouse.fr.

That is, besides the bifurcations occurring in smooth systems, the new element introduced by the piecewise definition leads to the so-called border collision bifurcations (BCB for short). This term is now widely used since its introduction in Refs. 13 and 14 in discrete systems, to which we are interested in. A border collision of an attracting set occurs whenever the invariant set collides with the border, as crossing the border the system changes definition. It has been shown that such bifurcations can lead to atypical transitions; for example, a fixed point can directly bifurcate into a periodic orbit of any period or cyclical chaotic intervals of any period. Many examples have been studied in the last years. In a piecewise linear one-dimensional system, the direct transition of a stable fixed point to a cycle of any period or to chaos has been shown, for example, in Refs. 15–17, and similar bifurcations in one-dimensional piecewise smooth systems are shown in Refs. 18 and 19. In two-dimensional systems, the spectrum of dynamic occurrences is much wider, and the subject is still to be completely studied. A two-dimensional map in canonical form is investigated in Refs. 13 and 20–22 and the transitions to torus or mode locking regimes in Refs. 23–25.

However, the results in piecewise smooth systems are only a few, and each system to be investigated may lead to new bifurcation phenomena. This is not the case in our piecewise smooth system. In fact, in this paper, we shall propose a quite simple circuit (similar to those proposed in Refs. 26 and 27), which is ultimately described by a piecewise smooth two-dimensional map. A particular case of the circuit, in which the system becomes piecewise linear, has been already studied in Ref. 28. Now we consider another simplified case of the general model, which leads to a piecewise smooth map, which is described in Sec. II. In this study, we give a complete characterization of the possible dynamics, and the analysis here performed may be of help in other similar models.

The model here considered can be analytically investigated due to the structure of the so-called triangular form of the system. The systems of this kind, although two-dimensional, keep many properties as those of the one-dimensional ones.^{29–31} Moreover, the driving function is one-dimensional and piecewise linear so that the complete analysis of our system can be performed making use of the results of the skew-tent map, already well studied since many years.^{14,15,32} We shall recall these results in Appendix A, because they are used to find the analytic expressions of the bifurcations curves occurring in our two-dimensional piecewise smooth system. In Appendix B, we also recall some properties of a two-dimensional system in triangular form, which are used and improved, in our specific case.

The rest of the paper is as follows. In Sec. II, we illustrate the circuit, which is ultimately described by a two-dimensional model that maps the unit square into itself and defined via three different continuous functions. We shall consider the model under a specific assumption, whose generic properties are described in Sec. II A, and the new results are presented in Secs. III and IV. In Sec. III, we show that the analysis of the bifurcations occurring in the piece-

wise smooth map can be performed either reducing the system to a one-dimensional skew-tent map f or to a two-dimensional piecewise smooth system in triangular form, in which the one-dimensional function is topologically conjugate to the same skew-tent map f . This allows us to prove all the main results of the piecewise smooth system. In Sec. IV, we show that all the stable cycles that the system can have undergo a degenerate flip bifurcation,³⁶ which also can be analytically detected. This means that a stable cycle of double period is not created close to the bifurcation cycle. We shall see that apart from the fixed point, any other stable k -cycle, for any $k \geq 2$, bifurcates directly to cyclical chaotic sets. The ranges in the parameter space at which the dynamics are chaotic are analytically determined, via the homoclinic bifurcations leading to chaotic sets in one piece. That is, we prove rigorously that the attracting chaotic set of positive measure is robust and in which regions it occurs. Section V concludes.

II. DESCRIPTION OF THE CIRCUIT

As already remarked in Sec. I, chaotic signals are very useful in many applications, specially in communications, and there are many implementations of chaos generators in the literature. Some of them operate in continuous time such as systems based on the Chua's circuit (analog circuit), while others are discrete time systems that iterate a chaotic map.

The model here proposed as chaos generator is a quite simple circuit, very similar to those discussed in Refs. 26 and 27. The main difference is in the use of two coupled state variables, leading to a two-dimensional map.

The proposed circuit is shown in Fig. 1 and consists of an R-S flip-flop, which permits to change the position of two switches simultaneously. Depending on the position “1” or “0” of the switches, two capacitor–resistance circuits C_x – R_x and C_y – R_y are supplied with dc voltage sources V_x and V_y , respectively, or connected to the ground. State variables of the system are the two voltages across the capacitors $v_x(t)$ and $v_y(t)$. At every clock period T , the flip-flop is set and then the switches position is “1.” When one of the voltages reaches the reference value V_{ref} , the two switches are turned

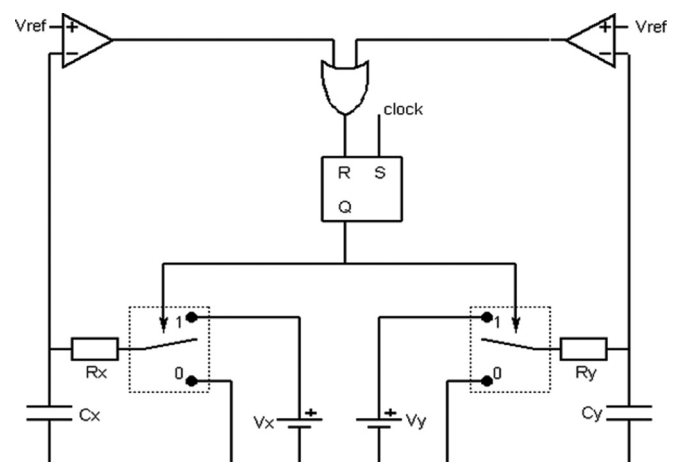


FIG. 1. Schematic picture of the circuit, describing an R-S flip-flop, which permits to change the position of two switches simultaneously.

toward their position “0.” So, according to the switches position, the two capacitors are simultaneously charging or discharging.

At the n th rising edge of the clock, the two state variables are given by $v_x(nT)$ and $v_y(nT)$, and the capacitors start charging. Then, it requires the duration $t_x^{(n)} = R_x C_x \ln([V_x - v_x(nT)]/[V_x - V_{ref}])$ to the voltage $v_x(t)$ to reach V_{ref} , and similarly, it requires the duration $t_y^{(n)} = R_y C_y \ln([V_y - v_y(nT)]/[V_y - V_{ref}])$ to the voltage $v_x(t)$ to reach V_{ref} . Then, three cases can happen:

1. None of the two states variables have reached the reference voltage V_{ref} before the next rising edge of the clock. This case appears when $t_x^{(n)} < T$ and $t_y^{(n)} < T$ or, equivalently, when $v_x(nT) < V_x - (V_x - V_{ref})e^{T/R_x C_x}$ and $v_y(nT) < V_y - (V_y - V_{ref})e^{T/R_y C_y}$. Then no switch has occurred, and the values of the state variables at the $(n + 1)$ th rising edge are

$$\begin{cases} v_x((n + 1)T) = V_x + (v_x(nT) - V_x)e^{-(T/R_x C_x)} \\ v_y((n + 1)T) = V_y + (v_y(nT) - V_y)e^{-(T/R_y C_y)} \end{cases} \quad (1)$$

2. Voltage $v_x(t)$ reaches the reference voltage V_{ref} before $v_y(t)$ can do it and before the next rising edge. It happens when $v_x(nT) \geq V_x - (V_x - V_{ref})e^{T/R_x C_x}$ and when $t_x^{(n)} \leq t_y^{(n)}$. Then the two switches are turned to “0” at time $nT + t_x^{(n)}$, and the values of the state variables at the $(n + 1)$ th rising edge are

$$\begin{cases} v_x((n+1)T) = V_{ref} \frac{V_x - v_x(nT)}{V_x - V_{ref}} e^{-(T/R_x C_x)}, \\ v_y((n+1)T) = \left(V_y \left(\frac{V_x - v_x(nT)}{V_x - V_{ref}} \right)^{R_x C_x / R_y C_y} - V_y + v_y(nT) \right) e^{-(T/R_y C_y)}. \end{cases} \quad (2)$$

3. Voltage $v_y(t)$ reaches the reference voltage V_{ref} before the next rising edge. This case is the analogous of the previous one. It happens when $v_y(nT) \geq V_y - (V_y - V_{ref})e^{T/R_y C_y}$ and when $t_x^{(n)} \geq t_y^{(n)}$. Then the two switches are turned to “0” at time $nT + t_y^{(n)}$, and the values of the state variables at the $(n + 1)$ th rising edge are

$$\begin{cases} v_x((n+1)T) = \left(V_x \left(\frac{V_y - v_y(nT)}{V_y - V_{ref}} \right)^{R_y C_y / R_x C_x} - V_x + v_x(nT) \right) e^{-(T/R_x C_x)}, \\ v_y((n+1)T) = V_{ref} \frac{V_y - v_y(nT)}{V_y - V_{ref}} e^{-(T/R_y C_y)}. \end{cases} \quad (3)$$

The normalized parameters of the model are defined as

$$\begin{aligned} \alpha &= \frac{V_x}{V_{ref}} > 1, \quad \alpha\rho = \frac{V_y}{V_{ref}} > 1, \quad \rho > 0, \quad \mu = \frac{R_y C_y}{R_x C_x} > 0, \\ \delta &= e^{-(T/R_x C_x)} \in (0, 1). \end{aligned} \quad (4)$$

The normalized state variables are given by

$$x_n = \frac{v_x(nT)}{V_{ref}} \in [0, 1], \quad y_n = \frac{v_y(nT)}{V_{ref}} \in [0, 1]. \quad (5)$$

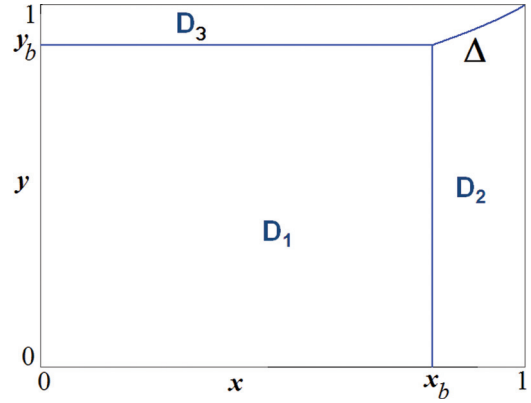


FIG. 2. (Color online) Phase space Q and three different regions D_i as defined in the text, in which the map is described by the different functions M_i or T_i .

The following switching curves in $Q = [0, 1] \times [0, 1]$:

$$\begin{aligned} x &= x_b, \quad x_b = \alpha - \frac{\alpha - 1}{\delta}, \\ y &= y_b, \quad y_b = \alpha\rho - \frac{\alpha\rho - 1}{\delta^{1/\mu}}, \end{aligned} \quad (6)$$

$$\Delta(x, y) = 0, \quad \Delta(x, y) = \left(\frac{\alpha\rho - y}{\alpha\rho - 1} \right)^\mu - \frac{\alpha - x}{\alpha - 1},$$

assuming $x_b \geq 0$ and $y_b \geq 0$, which occurs for

$$\bar{\delta} < \delta < 1, \quad \bar{\delta} = \max \left\{ \frac{\alpha - 1}{\alpha}, \left(\frac{\alpha\rho - 1}{\alpha\rho} \right)^\mu \right\}, \quad (7)$$

define three different domains in Q (see Fig. 2):

$$\begin{aligned} D_1 &= \{(x, y) \mid 0 \leq x \leq x_b \text{ and } 0 \leq y \leq y_b\}, \\ D_2 &= \{(x, y) \mid x_b \leq x \leq 1 \text{ and } \Delta(x, y) \geq 0\}, \\ D_3 &= \{(x, y) \mid y_b \leq y \leq 1 \text{ and } \Delta(x, y) \leq 0\}, \end{aligned} \quad (8)$$

in which the system is defined by different functions. In fact, the circuit is modeled by the continuous map $(x_{n+1}, y_{n+1}) = M(x_n, y_n)$ as follows:

if $(x_n, y_n) \in D_1$:

$$M(x_n, y_n) = M_1(x_n, y_n) = \begin{cases} \alpha + (x_n - \alpha)\delta \\ \alpha\rho + (y_n - \alpha\rho)\delta^{1/\mu} \end{cases}$$

if $(x_n, y_n) \in D_2$:

$$M(x_n, y_n) = M_2(x_n, y_n) = \begin{cases} \frac{\alpha - x_n}{\alpha - 1} \delta \\ \left(\alpha\rho \left(\frac{\alpha - x_n}{\alpha - 1} \right)^{1/\mu} - \alpha\rho + y_n \right) \delta^{1/\mu} \end{cases}$$

if $(x_n, y_n) \in D_3$:

$$M(x_n, y_n) = M_3(x_n, y_n) = \begin{cases} \left(\alpha \left(\frac{\alpha\rho - y_n}{\alpha\rho - 1} \right)^\mu - \alpha + x_n \right) \delta \\ \left(\frac{\alpha\rho - y_n}{\alpha\rho - 1} \right) \delta^{1/\mu} \end{cases}. \quad (9)$$

It is easy to see that the map is well defined as it is continuous and maps the square Q (the phase space of interest) into itself.

The analysis of the dynamics of this model as a function of the four parameters $(\alpha, \rho, \delta, \text{ and } \mu)$ is not an easy task. The particular case, with $\mu = 1$ fixed, as a function of $(\alpha, \rho, \text{ and } \delta)$ has been studied in Ref. 25. There it has been shown that map M becomes *piecewise linear*, and the bifurcations of the model and route to chaos could be well determined.

In this work, another special configuration of this circuit will be studied, the one in which $V_x = V_y$, that means, $\rho = 1$, so that the considered circuit, depending on the parameters $(\alpha, \delta, \text{ and } \mu)$, is modeled by the following *piecewise smooth* map $(x_{n+1}, y_{n+1}) = T(x_n, y_n)$:

if $(x_n, y_n) \in D_1$:

$$T(x_n, y_n) = T_1(x_n, y_n) = \begin{cases} \alpha + (x_n - \alpha)\delta \\ \alpha + (y_n - \alpha)\delta^{1/\mu}, \end{cases}$$

if $(x_n, y_n) \in D_2$:

$$T(x_n, y_n) = T_2(x_n, y_n) = \begin{cases} \frac{\alpha - x_n}{\alpha - 1} \delta \\ \left(\alpha \left(\frac{\alpha - x_n}{\alpha - 1} \right)^{1/\mu} - \alpha + y_n \right) \delta^{1/\mu}, \end{cases}$$

if $(x_n, y_n) \in D_3$:

$$T(x_n, y_n) = T_3(x_n, y_n) = \begin{cases} \left(\alpha \left(\frac{\alpha - y_n}{\alpha - 1} \right)^\mu - \alpha + x_n \right) \delta \\ \left(\frac{\alpha - y_n}{\alpha - 1} \right) \delta^{1/\mu} \end{cases}. \quad (10)$$

These two cases (the one studied in Ref. 25 and the one here considered), which are simpler, constitute a first step toward the understanding of the dynamics of the general model, as a function of all four the parameters.

A. General properties

Although the map T under study is now piecewise smooth, we can prove the occurrence of bifurcation structures similar to those detected in Ref. 28 for the piecewise linear case. We shall see that, in the phase space Q , only two domains among the three cases are involved (either D_1 and D_2 or D_1 and D_3), leading to a simplified system whose bifurcation structure can be fully analyzed in the parameter space, while in the general model (9), all the three domains can be involved leading to more complex regions in the parameter space.

The analysis of the bifurcations occurring in the piecewise smooth map T given above, depending on three parameters α, δ , and μ , can be performed in a few steps. In Sec. III, we shall describe that we can consider three different regimes, characterized by different values of the parameter μ , that is, $\mu = 1, \mu > 1$, and $\mu < 1$.

Fixing $\mu = 1$, we shall see that the asymptotic dynamics of the two state variables (x_n, y_n) are synchronized, that is, $x_n = y_n$, and all the bifurcations [in the parameter plane (α, δ)] are completely described by a one-dimensional map f topologically conjugate to the skew-tent map (recalled in Appendix A).

Then we shall show that the two cases $\mu > 1$ and $0 < \mu < 1$ are topologically conjugate to one another. In Sec. IV, we shall consider the case $\mu > 1$, showing that the dynamics are confined to two regions only, D_1 and D_2 , and the functions involved, T_1 and T_2 , lead to a map that has a triangular structure (recalled in Appendix B). In fact, as we can see from their definition, the value of x_{n+1} depends only on x_n , and this will lead to a simplified system, whose bifurcations can also be determined via the same one-dimensional piecewise linear function f conjugate to the skew-tent map

and can be completely determined (for any value of μ) in the parameter plane (α, δ) .

We shall see that stable cycles of any period can exist, describing the related route to chaos. As the model is piecewise smooth, we could expect flip bifurcations of supercritical or subcritical type, in which cycles of double period exist close to the bifurcating cycles. Instead, these properties described above lead to the unexpected result that all the flip bifurcations of the existing stable k -cycles are degenerate. This means that at the flip bifurcation value, in any neighborhood of the bifurcating cycle, we can find a smooth arc with infinitely many cycles of double period and that, after the flip bifurcation, a stable cycle of double period does not exist close to the bifurcating one. Instead, for $k=1$, a stable 2-cycle appears *far from* the bifurcating fixed point (with periodic point in two different regions), while for any $k > 1$ after the flip bifurcation *no stable $2k$ -cycles exist*, instead the bifurcation leads directly to robust chaos in cyclical sets.

In general, for piecewise smooth maps, it is difficult to have the analytic expression of the bifurcations curves in the parameter plane leading to chaos, and also the chaotic regime is usually proved numerically, often via the Lyapunov exponents. Differently, the main results in this paper are that we can detect the analytical expression of all the bifurcations (both associated with the existence of stable cycles and associated with the transition to chaos in cyclical chaotic sets) and that we can rigorously prove that the chaotic regime is always purely chaotic and persistent under parameter variation. These results are possible due to the triangular structure of the map T under study in all the cases $\mu = 1, \mu > 1$, and $\mu < 1$, coupled with the one-dimensional map f conjugate to the skew-tent map.

III. ANALYSIS OF THE DYNAMIC PROPERTIES OF T

In this section, we prove the dynamic properties remarked above, occurring in the circuit modeled by T given in Eqs. (10) and (8). The model is described by a continuous piecewise smooth map depending on three parameters α, δ , and μ , under the constraints given in Eqs. (4) and (7). Of the three functions involved in Eq. (10), it is immediate to see that T_1 is linear, and its fixed point, say $X_1^* = (x_1^*, y_1^*) = (\alpha, \alpha)$, is outside the square Q (as $\alpha > 1$), and thus it is a so-called virtual fixed point. Moreover, the eigenvalues of T_1 are both positive and less than 1, so the virtual fixed point is a stable node. This implies that initial conditions inside the region D_1 are mapped toward the virtual attractor and are forced to enter in a different region, either D_2 or D_3 , from which the iterated points are kept inside Q .

The fixed points of the system inside Q are given by the functions T_2 and T_3 , say X_2^* and X_3^* , respectively, and they never occur simultaneously. In fact, as we shall see below, for $\mu > 1$, the fixed point X_2^* exists in the proper region D_2 while X_3^* is virtual, and vice versa, for $0 < \mu < 1$, the fixed point X_3^* exists in the proper region D_3 while X_2^* is virtual.

Moreover, we shall see that this distinction in the existence of the fixed points also persists in the dynamics occurring in the phase space. When X_2^* exists, then the dynamics involve only the regions D_1 and D_2 (for $\mu > 1$).

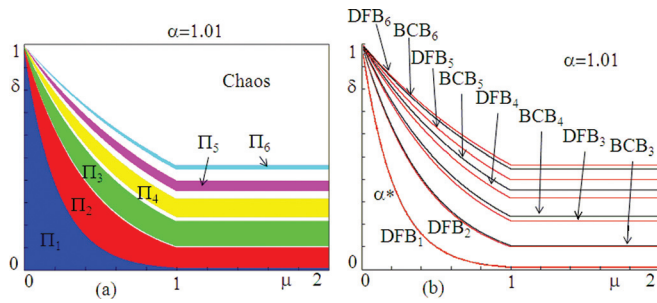


FIG. 3. (Color online) Bifurcation diagram in the parameter plane (μ, δ) at $\alpha = 1.01$ fixed, for the map T in Eq. (10). In (a), the colored regions Π_k denote the existence of stable k -cycles. The white region denotes chaos. In (b) are shown a few bifurcation curves described in Sec. IV. BCB_k are border collision bifurcation curves for k -cycles, while DFB_k denotes a degenerate flip bifurcation curve of a stable k -cycle.

Alternatively, when X_3^* exists, then the dynamics involve only the regions D_1 and D_3 (for $\mu < 1$).

A two-dimensional bifurcation diagram as in Fig. 3 immediately illustrates a qualitative change in the dynamic structure. Figure 3(a) shows a two-dimensional bifurcation diagram in the parameter plane (μ, δ) obtained via numerical computations at $\alpha = 1.01$ fixed. Periodicity regions Π_k of attracting cycles of increasing period k are evidenced in different colors. We can see a difference between the region in $\mu > 1$ and that in $\mu < 1$. This different dynamic behavior in the two regimes $\mu > 1$ and that in $\mu < 1$ will be explained below in Proposition 2.

Let us first analyze what occurs at the separating value $\mu = 1$. From the definition of the model, we can see that the value $\mu = 1$ is particular, as the map from piecewise smooth becomes piecewise linear. Moreover, we can prove that both the state variables tend to synchronized states, as both tend to be equal, thus belonging to the diagonal Δ of the phase space Q . The restriction of the map to the diagonal Δ is a piecewise linear map topologically conjugate to the skew-tent map. We prove the following result:

Proposition 1: Let $\mu = 1$. Then the dynamics of the model in the phase space Q converges to the diagonal, and the dynamics of $x_n = y_n$ are topologically conjugate to those of the skew-tent map

$$f : X \mapsto f(X) = \begin{cases} f_L(X) = \delta X + 1, & X \leq 0 \\ f_R(X) = -\frac{\delta}{\alpha - 1} X + 1, & X \geq 0 \end{cases} \quad (11)$$

via the change of variable $X = \delta(x - x_b)/[(\alpha - 1)(1 - \delta)]$.

The proof of Proposition 1 comes via the following steps.

- (i) The fixed point of the map is given by $X_2^* = X_3^* = (\alpha\delta/(\alpha + \delta - 1), \alpha\delta/(\alpha + \delta - 1))$, which belongs to the diagonal. The switching set $\Delta(x, y) = 0$ also belongs to the diagonal, so that the fixed point is on the boundary of the regions D_2 and D_3 .
- (ii) The regions below (respectively, above) the diagonal are invariant. In fact, the diagonal itself is invariant, being the eigenvector of the linear maps. While considering a point $(x, y) \in D_1$ below (respectively, above) the diagonal, it is mapped in a few iterations in

the region D_2 (respectively, D_3). Now, considering a point $(x_n, y_n) \in D_2$, thus below the diagonal, satisfying $y_n < x_n$, we get $y_{n+1} = \alpha\delta((\alpha - x_n)/(\alpha - 1)) - \alpha\delta + y_n < \alpha\delta((\alpha - x_n)/(\alpha - 1)) - \alpha\delta + x_n\delta = x_{n+1}$, which is a point still below the diagonal. Similarly, if we consider $(x_n, y_n) \in D_3$, above the diagonal, then also (x_{n+1}, y_{n+1}) is above the diagonal.

- (iii) The iterations of the map below the diagonal are such that $(x_{n+1} - y_{n+1}) = \delta(x_n - y_n)$, both applying the map T_1 and the map T_2 , thus the asymptotic state, as $n \rightarrow \infty$, belongs to the diagonal. Similarly, for points above the diagonal, they converge to the diagonal.
- (iv) The asymptotic behavior of the map below the diagonal is given by the two functions T_1 and T_2 leading to

$$x_{n+1} = \begin{cases} \delta x_n + \alpha(1 - \delta), & x_n \leq x_b = \alpha - \frac{\alpha - 1}{\delta} \\ -\frac{\delta}{\alpha - 1} x_n + \frac{\alpha\delta}{\alpha - 1}, & x_n \geq x_b, \end{cases} \quad (12)$$

and with the change of variable $X = \delta(x - x_b)/[(\alpha - 1)(1 - \delta)]$, the map in Eq. (11) is obtained. Similarly, the asymptotic behavior of the map above the diagonal is given by the two functions T_1 and T_3 leading to the same steps as above with x replaced by y , which ends the proof. \square

The dynamic behaviors of the skew-tent map are well known, and the results associated with our model are useful not only in this particular case $\mu = 1$ but also in Sec. IV, for the piecewise smooth model. So the dynamics of this map are reported in Appendix A for the parameter ranges of interest: $0 < a = \delta < 1$ and $b = -\delta/(\alpha - 1) < 0$.

Given the benchmark case occurring at $\mu = 1$, we shall see that it is enough to study one case only ($\mu > 1$ or $\mu < 1$). In fact, the following property holds:

Proposition 2: The two cases $\mu > 1$ and $\mu < 1$ are topologically conjugate.

The proof follows immediately via a change of variable, substituting (x, y, δ, μ) with $(y, x, \delta^{1/\mu}, 1/\mu)$ as

$$\begin{aligned} T_1(x_n, y_n, \delta, \mu) &= T_1(y_n, x_n, \delta^{1/\mu}, 1/\mu), \\ T_2(x_n, y_n, \delta, \mu) &= T_3(y_n, x_n, \delta^{1/\mu}, 1/\mu), \end{aligned} \quad (13)$$

which can be immediately verified.

Due to the topological conjugation of the two different regimes, in the following, we can restrict our analysis to only one of them. In Sec. IV, we shall completely describe the dynamics in the regime $\mu > 1$.

IV. PIECEWISE SMOOTH MAP T FOR $\mu > 1$

In this section, we consider the parameter $\mu > 1$ showing that the dynamics of the piecewise smooth map T defined in three pieces are reduced to those of a piecewise smooth map T defined in two pieces, which is in triangular form, and we shall prove that the bifurcation structures are strictly related to those of a one-dimensional piecewise linear map. This will lead us to determine the analytic expression of the bifurcation curves associated with the stable cycles as well as those associated with the homoclinic bifurcations of repelling cycles leading to robust chaos, proving that the chaotic regime is always persistent as a function of the parameters. Thus,

differently from what generally occurs in piecewise smooth models, we have a complete description in the parameter space of the values, which are associated with a stable (attracting) cycle or with chaos, whose structural stability is also proved.

From the definition of T , we can see that, for $\mu > 1$, only two regions of the phase space Q are involved in the asymptotic dynamics. In fact, from the definition of the constraints, we have $y_b > x_b$, so that the point (x_b, y_b) is above the diagonal of Q , as well as the curve of equation $\Delta(x, y) = 0$ bounding from above the region D_2 . The fixed point of the model is given by

$$X_2^* = (x_2^*, y_2^*) = \left(\frac{\alpha\delta}{\delta + \alpha - 1}, \left(\left(\frac{\alpha}{\delta + \alpha - 1} \right)^{1/\mu} - 1 \right) \frac{\alpha\delta^{1/\mu}}{1 - \delta^{1/\mu}} \right) \in D_2, \tag{14}$$

while X_3^* is virtual. Any initial condition in the region D_3 will be mapped into $D_1 \cup D_2$ in a finite number of iterations (as the points tend to the virtual fixed point X_3^* , which is either attracting or a saddle). Any initial condition $(x_n, y_n) \in D_1$ under the map T_1 is attracted by a virtual fixed point $X_1^* = (\alpha, \alpha)$ belonging to the diagonal and will be mapped into D_2 in a finite number of steps. Points in D_2 are subject to the function T_2 , which is a triangular map with a linear function $F(x_n) = -[\delta/(\alpha - 1)]x_n + [\alpha\delta/(\alpha - 1)]$ in the autonomous state variable, while $G(x_n, y_n) = (\alpha[(\alpha - x_n)/(\alpha - 1)]^{1/\mu} - \alpha + y_n)\delta^{1/\mu}$ is a contraction in the y -direction.

In Subsection IV A, we show that when X_2^* is locally stable, then it is also globally attracting in the phase space Q , and it becomes unstable via a degenerate flip bifurcation, which leads to an attracting 2-cycle having the two periodic points in the two different domains D_1 and D_2 .

Then in Subsection IV B, we prove that when the fixed point is unstable the dynamics of T , confined in the region $D_1 \cup D_2$, are determined by a piecewise smooth map in triangular form, in which the independent variable x_n is related with a one-dimensional piecewise linear map, which is the same function f determined in Eq. (11). So, we can prove that all the cycles of f are also associated with cycles of the piecewise smooth map T (which is not a common occurrence in triangular maps). In our model, this is due to the particular form of the second function depending on (x_n, y_n) . This allows us to say that all the bifurcations of map T associated with the appearance/disappearance of a k -cycle are border collision bifurcations, denoted as BCB_k , and that a stable cycle can become unstable only via a degenerate flip bifurcation, denoted as DFB_k . Moreover, we can completely describe the structure of the chaotic sets. In fact, for any $k \geq 3$, crossing the curve BCB_k , a pair of cycles exists, q_k and q'_k ; q_k may be stable and q'_k is unstable. Then, decreasing α ,

- (i) the stable k -cycle q_k becomes unstable crossing the curve DFB_k , leading to $2k$ -cyclical chaotic sets;
- (ii) the $2k$ -cyclical chaotic sets become k -cyclical chaotic sets at the first homoclinic bifurcation of q_k (which occurs crossing the bifurcation curve H_k);

- (iii) the k -cyclical chaotic intervals turn into one-piece chaotic intervals at the first homoclinic bifurcation of q'_k (which occurs crossing the bifurcation curve H'_k).

All the bifurcation curves here involved will be analytically determined.

We have not mentioned above the 2-cycle. Indeed, it is particular. Its route is different from those of the k -cycles with $k \geq 3$. In fact, it is not related with an unstable 2-cycle but only to the fixed point X_2^* . A 2-cycle can appear only via the degenerate flip bifurcation of the fixed point, crossing the curve DFB_1 , and on its turn, it becomes unstable via degenerate flip bifurcation crossing the curve DFB_2 . However, when the 2-cycle becomes unstable, a stable cycle of double period can never appear, and the resulting dynamics depend on the crossing point of the curve DFB_2 . The widest arc leads the dynamics to 4-cyclical chaotic sets; nevertheless, it is also possible to get a transition to any kind of 2^m -cyclical chaotic sets, for any $m \geq 2$.

A. Fixed point

From the property of the function T_2 defined in D_2 , where the fixed point X_2^* exists, we prove that as long as the fixed point X_2^* is locally stable, then it is also globally attracting in the phase space Q . As remarked above, T_2 is triangular, thus any cycle of T_2 is associated with a cycle of the function $F(x_n) = -[\delta/(\alpha - 1)]x_n + [\alpha\delta/(\alpha - 1)]$ in the autonomous state variable, while the vice versa is not necessarily true. However, in our case, the simple structure of the second function $G(x_n, y_n) = (\alpha[(\alpha - x_n)/(\alpha - 1)]^{1/\mu} - \alpha + y_n)\delta^{1/\mu}$ leads to the result that also any cycle of the function $F(x_n)$ leads to a cycle of T_2 . In fact, for any fixed value of x , say \bar{x} , the function G is linear in y :

$$G(\bar{x}, y) = y\delta^{1/\mu} + \left(\alpha \left(\frac{\alpha - \bar{x}}{\alpha - 1} \right)^{1/\mu} - \alpha \right) \delta^{1/\mu}, \tag{15}$$

and a contraction in the y -direction, as $\lambda_2 = \delta^{1/\mu} \in (0, 1)$.

So, for the fixed point X_2^* , the eigenvalues of the Jacobian matrix DT_2 are given by

$$\lambda_1 = -\frac{\delta}{\alpha - 1}, \quad \lambda_2 = \delta^{1/\mu}, \tag{16}$$

where $\lambda_2 \in (0, 1)$ by assumption, and its associated eigenvector, the vertical line through the fixed point, is always a stable eigenspace. While the eigenvalue λ_1 is negative and a bifurcation occurs to X_2^* when λ_1 crosses, the value -1 at

$$\alpha^* = 1 + \delta. \tag{17}$$

Thus for $\alpha > \alpha^*$, the fixed point X_2^* is globally attracting.

We have now to see what occurs at the bifurcation value $\alpha = \alpha^*$. For a linear one-dimensional map, we know that the flip bifurcation occurring when λ_1 crosses the value -1 is a degenerate flip bifurcation: at the bifurcation, apart from the fixed point, we have all cycles of period 2, stable but not asymptotically stable, and divergence after. This is reflected also in our triangular map T_2 . In fact, in our case, the first component $F(x)$ is linear, so that, at the bifurcation value, we have a segment filled with 2-cycles, and, as proved above,

any cycle of the function $F(x)$ also leads to a cycle of T_2 . That is, if $\{x_1, x_2\}$ is a 2-cycle of $F(x)$, then a 2-cycle

$$\{(x_1, G(x_1, y_1)), (x_2, G(x_2, y_2))\} \quad (18)$$

of T_2 also exists. We have so proved that the flip bifurcation occurring at the fixed point X_2^* is degenerate.³⁸ This is not a common occurrence. Moreover, in Subsection IV B, we shall see that *all the attracting k-cycles* of the piecewise smooth map T under study undergo only degenerate flip bifurcations.

In our case, the map T_2 is defined in the region D_2 and, at the degenerate flip bifurcation value occurring at $\alpha = \alpha^*$ the whole segment $[x_b, 1]$, where $x_b = \delta$, is filled with 2-cycles of the linear map $F(x)$ so that also the map T_2 must have an invariant smooth arc in the region D_2 , which is filled with 2-cycles of the map T , with x ranging in the whole segment $[x_b, 1]$ defining the region D_2 . All these 2-cycles (stable but not asymptotically stable) have a stable set on the vertical lines through the cycles. An example is shown in Fig. 4.

We have so proved the following:

Proposition 3: Let $\mu > 1$ and $\alpha > \alpha^ = 1 + \delta$. Then T has the fixed point X_2^* globally attracting in the state space Q . At $\alpha = \alpha^*$, a degenerate flip bifurcation occurs and an arc of invariant curve crosses the region D_2 filled with stable 2-cycles, transversely attracting.*

The line of equation $\alpha = 1 + \delta$ is shown in the bifurcation diagram of Fig. 5, in the two-dimensional parameter plane (α, δ) . Note that due to the constraint $\bar{\delta} < \delta < 1$, we necessarily have $1 < \alpha < 2$. We also remark that at any fixed value $\mu > 1$, the bifurcation diagram in the parameter plane (α, δ) is the same because, as we have seen for $\alpha = 1 + \delta$, also all the other bifurcations curves are independent of the parameter μ . This will be shown in Subsection IV B, together with the description of the dynamics occurring for $\alpha < \alpha^*$.

B. Stable k-cycles and chaos

It is clear that for $\alpha < \alpha^* = 1 + \delta$, we can no longer have an attractor only in the region D_2 as points not belonging to the vertical line through the saddle fixed point X_2^* are necessarily mapped into the region D_1 . Thus, the model becomes really piecewise smooth: the asymptotic states are

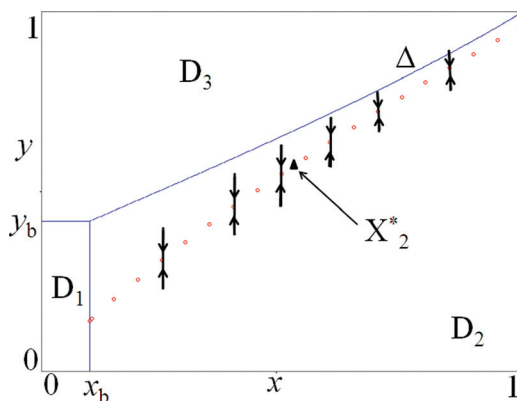


FIG. 4. (Color online) Degenerate flip bifurcation of X_2^* at the parameter values $\delta = 0.1, \alpha = \alpha^* = 1.1, \mu = 1.2$. Only a few 2-cycles are shown in the figure, with their transversal stable sets.

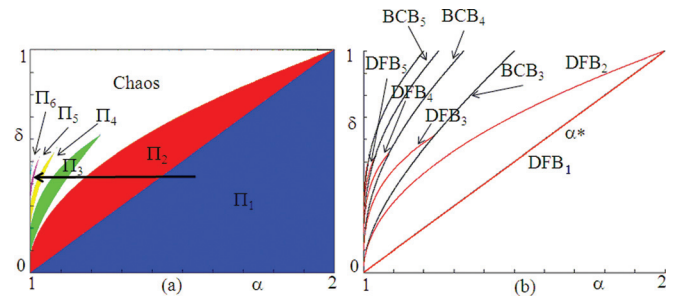


FIG. 5. (Color online) Bifurcation diagram in the parameter plane (α, δ) (for any $\mu > 1$) for the map T in Eq. (10). In (a), the colored regions Π_k denote the existence of stable k -cycles. The white region denotes chaos. In (b) are shown a few bifurcation curves, whose analytic equations are given in Sec. IV B.

confined in the region $D_1 \cup D_2$, and the dynamics of the map T are described by the interaction of the two maps T_1 and T_2 . That is, for $1 < \alpha < \alpha^*$, our map T is determined by

if $(x_n, y_n) \in D_1$:

$$T(x_n, y_n) = T_1(x_n, y_n) = \begin{cases} \alpha + (x_n - \alpha)\delta \\ \alpha + (y_n - \alpha)\delta^{1/\mu} \end{cases}$$

if $(x_n, y_n) \in D_2$:

$$T(x_n, y_n) = T_2(x_n, y_n) = \begin{cases} \frac{\alpha - x_n}{\alpha - 1} \delta \\ \left(\alpha \left(\frac{\alpha - x_n}{\alpha - 1} \right)^{1/\mu} - \alpha + y_n \right) \delta^{1/\mu} \end{cases} \quad (19)$$

However, as already remarked, also now we are dealing with a map in triangular form. In fact, map T is in the form $x_{n+1} = F(x_n), y_{n+1} = G(x_n, y_n)$ with the following definitions:

$$F(x_n) = \begin{cases} \delta x_n + \alpha(1 - \delta), & x_n \leq x_b = \alpha - \frac{\alpha - 1}{\delta} \\ -\frac{\delta}{\alpha - 1} x_n + \frac{\alpha \delta}{\alpha - 1}, & x_n \geq x_b \end{cases} \quad (20)$$

$$G(x_n, y_n) = \begin{cases} \delta^{1/\mu} y_n + \alpha(1 - \delta^{1/\mu}), & x_n \leq x_b = \alpha - \frac{\alpha - 1}{\delta} \\ \left(\alpha \left(\frac{\alpha - x_n}{\alpha - 1} \right)^{1/\mu} - \alpha + y_n \right) \delta^{1/\mu}, & x_n \geq x_b \end{cases} \quad (21)$$

Thus, for this triangular map, we can appreciate the importance of the piecewise linear map $F(x)$ in Eq. (20), which is a skew-tent map with critical point in $x = x_b$. Moreover, we can reason as we have done before for the triangular map T_2 because also now the dependent function $G(x, y)$ is linear with respect to the variable y , and $\lambda_2 = (\partial/\partial y)G(x, y) = \delta^{1/\mu}$ is a contraction factor. It follows that not only any cycle of T is associated with a cycle of F (which is a generic property of a triangular map) but also the vice versa holds (which is not a common occurrence), so that we have the following:

Proposition 4: Let $\mu > 1$ and $1 < \alpha < \alpha^ = 1 + \delta$. Then $\{(x_i, y_i)\}_{i=1, \dots, k}$ is a k -cycle of T iff $\{x_i\}_{i=1, \dots, k}$ is a k -cycle of the skew-tent map $F(x)$ given in Eq. (20).*

It is clear that this is an important result that allows us to completely describe the bifurcations occurring in our model T . In fact, now we have that any cycle of F (and related bifurcations) leads to a companion cycle of T (and

related bifurcations), and the dynamic behaviors of the one-dimensional map in Eq. (20) are completely known: via the change of variables

$$\begin{aligned} X &= \frac{\delta}{(\alpha - 1)(1 - \delta)}(x - x_b) \\ &= \frac{\delta}{(\alpha - 1)(1 - \delta)}\left(x - \alpha + \frac{(\alpha - 1)}{\delta}\right), \\ Y &= \frac{\delta^{1/\mu}}{(\alpha - 1)(1 - \delta^{1/\mu})}(y - y_b) \\ &= \frac{\delta^{1/\mu}}{(\alpha - 1)(1 - \delta^{1/\mu})}\left(y - \alpha + \frac{(\alpha - 1)}{\delta^{1/\mu}}\right), \end{aligned} \tag{22}$$

we get the piecewise smooth system $(X_{n+1}, Y_{n+1}) = T(X_n, Y_n) = (f(X_n), \tilde{G}(X_n, Y_n))$, where

$$f(X_n) = \begin{cases} \delta X_n + 1, & X_n \leq 0, \\ -\frac{\delta}{\alpha - 1}X_n + 1, & X_n \geq 0, \end{cases} \tag{23}$$

$$\tilde{G}(X_n, Y_n) = \begin{cases} \delta^{1/\mu}Y_n + 1, & Y_n \leq 0, \\ B(1 - (1 - \delta)X)^{1/\mu} + \delta^{1/\mu}Y + 1 - B, & Y_n \geq 0, \end{cases} \tag{24}$$

and

$$B = \frac{\alpha\delta^{1/\mu}}{(\alpha - 1)(1 - \delta^{1/\mu})}. \tag{25}$$

The function in Eq. (23) is now the skew-tent map with slopes $a = \delta \in (\bar{\delta}, 1)$ and $b = -[\delta/(\alpha - 1)] < 0$ already defined in Eq. (11), whose dynamics and bifurcation curves are recalled in Appendix A. For values of $b \in (-1, 0)$, we get the dynamics already described: the map has the fixed point on the right side (corresponding to X_2^*) globally attracting. At $b = -1$, the degenerate flip bifurcation of the fixed point occurs. Now we can state that this bifurcation leads, for $b < -1$ (i.e., for $\alpha < \alpha^* = 1 + \delta$) to a stable 2-cycle for T with one periodic point in the region D_1 and one in the region D_2 . From Appendix A, we have the explicit expression of all the stable k -cycles, which the map $f(X_n)$ can have, and from the first equation in Eqs. (22), via the reverse function

$$x = \frac{(\alpha - 1)(1 - \delta)}{\delta}X + \alpha - \frac{(\alpha - 1)}{\delta}, \tag{26}$$

we get the explicit expressions for the x -coordinates of cycles for our map T in the region $D_1 \cup D_2$. For the 2-cycle, we have

$$X_R^2 = \frac{(1 + \delta)(\alpha - 1)}{\delta^2 + \alpha - 1}, \quad X_L^2 = \frac{\alpha - 1 - \delta}{\delta^2 + \alpha - 1}, \tag{27}$$

and thus

$$x_{D_2}^2 = \alpha - \frac{\alpha(\alpha - 1)\delta}{\delta^2 + \alpha - 1}, \quad x_{D_1}^2 = \frac{\alpha\delta^2}{\delta^2 + \alpha - 1}. \tag{28}$$

These are the x -coordinates of the 2-cycle of $f(X_n)$, but it is clear that we have to recover the second coordinate y of the cycle from our map T , and we obtain

$$\begin{aligned} y_{D_2}^2 &= \left(\alpha\delta^{2/\mu} \left(\left(\frac{\alpha - x_{D_2}^2}{\alpha - 1} \right)^{1/\mu} - 1 \right) + \alpha(1 - \delta^{1/\mu}) \right) / (1 - \delta^{2/\mu}), \\ y_{D_1}^2 &= \alpha\delta^{2/\mu} \left(\left(\frac{\alpha - x_{D_1}^2}{\alpha - 1} \right)^{1/\mu} - 1 \right) / (1 - \delta^{2/\mu}). \end{aligned} \tag{29}$$

The flip bifurcation of the fixed point and transition to a stable 2-cycle is shown in the one-dimensional bifurcation diagram of Fig. 6(a), obtained at fixed $\delta = 0.4$ and $\mu = 2$ [see the arrow in Fig. 5(a)], illustrating the x -variable as a function of α .

We remark that while the informations related with the coordinates of the stable k -cycles are only partially covered by the one-dimensional skew-tent map in (23) (as the y -coordinate is to be determined via the two-dimensional map T), the informations associated with the bifurcations are complete. Thus, all the bifurcations occurring in Fig. 6 as well as in Fig. 5 are analytically detected. In fact, from Proposition 4, we have that the bifurcations are only those occurring in the cycles of the map in Eq. (23). We have so proved (by using Appendix A) the following result:

Proposition 5: Let $\mu > 1$ and $1 < \alpha < \alpha^ = 1 + \delta$. Then*

- (i) *The stable 2-cycle of T undergoes a degenerate flip bifurcation, at the bifurcation curve given by*

$$\text{DFB}_2: \alpha = 1 + \delta^2, \tag{30}$$

which may lead to m -cyclical chaotic sets of any even period m , which undergo bifurcations, merging in pair, up to a one-piece chaotic set.

- (ii) *For any $k \geq 3$ pairs of k -cycles, one of which may be locally stable and one unstable, appear via border collision bifurcation crossing the bifurcation curve BCB_k given by*

$$\text{BCB}_k: \alpha = 1 + \frac{(1 - \delta)\delta^{k-1}}{1 - \delta^{k-1}}, \tag{31}$$

which are maximal cycles; the stable one has one periodic point in D_2 and $(k-1)$ points in D_1 ; the unstable one has two periodic points in D_2 and $(k-2)$ points in D_1 .

- (iii) *For any $k \geq 3$ the stable k -cycle undergoes a degenerate flip bifurcation at the bifurcation curve given by*

$$\text{DFB}_k: \alpha = 1 + \delta^k, \tag{32}$$

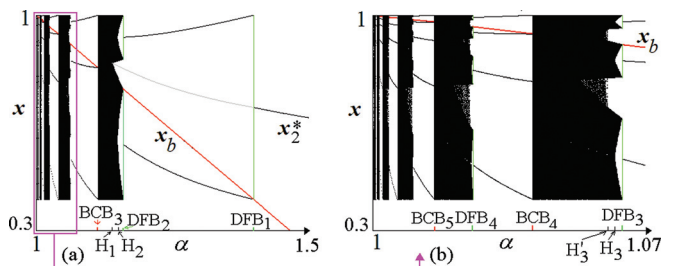


FIG. 6. (Color online) One-dimensional bifurcation diagram showing the x -coordinate as a function of the parameter α , at $\mu = 2$ and $\delta = 0.4$ fixed [see the arrow in Fig. 5(a)].

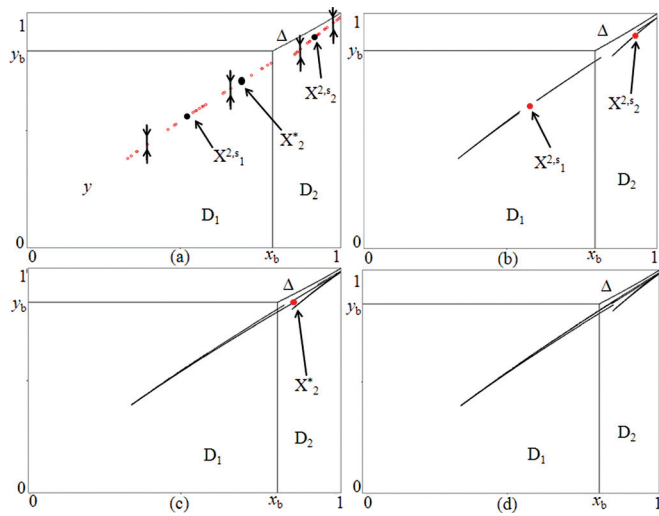


FIG. 7. (Color online) Phase space of T at the parameters $\alpha = 1.1$ and $\mu = 1.2$ fixed and $\delta = 0.316227766$ in (a), at the degenerate flip bifurcation of the 2-cycle, when infinitely many 4-cycles exist, some of which are shown, and the stable set of one 4-cycle is also plotted: $\delta = 0.323$ in (b); $\delta = 0.331$ in (c); $\delta = 0.332$ in (d).

so that the stability region of the k -cycle (colored regions in Fig. 5) is given by $(\alpha, \delta) \in \Pi_k$ where

$$\Pi_k = \left\{ (\alpha, \delta) \mid 1 + \delta^k < \alpha < 1 + \frac{(1 - \delta)\delta^{k-1}}{1 - \delta^{k-1}}, \bar{\delta} < \delta < 1 \right\}. \quad (33)$$

- (iv) Crossing the degenerate flip bifurcation DFB_k there is the appearance of $2k$ -cyclical chaotic sets, which merge into k -cyclical chaotic sets at the homoclinic bifurcation occurring at the bifurcation curve H_k given by

$$H_k: \alpha - \frac{\delta^{2k}}{(\alpha - 1)^2} = 0, \quad (34)$$

which in turn merge into one-piece chaotic sets at the homoclinic bifurcation occurring at the bifurcation curve H'_k given by

$$H'_k: \alpha - \frac{\delta^k}{(\alpha - 1)} = 0. \quad (35)$$

The shape of the periodicity region Π_k with stable k -cycles is shown in Fig. 5. In Fig. 5(b) are reported a few bifurcation curves determined analytically via the equations given above. We can see that fixing any value of δ , as α decreases from $\alpha^* = 1 + \delta$, a finite number of periodicity regions are crossed, and the lower is the δ , the higher the number of periodicity regions that are crossed. One transition is showed in Fig. 6. In Fig. 6(a), we can see that the bifurcation of the 2-cycle is followed by chaotic sets, 4-cyclical first, then 2-cyclical, and then in one piece. In the enlargement of Fig. 6(b), we can see the stable k -cycles, for $k = 3, 4, 5$, and 6, which are appearing via border collision from a chaotic set as α decreases, and all are followed by the same kind of

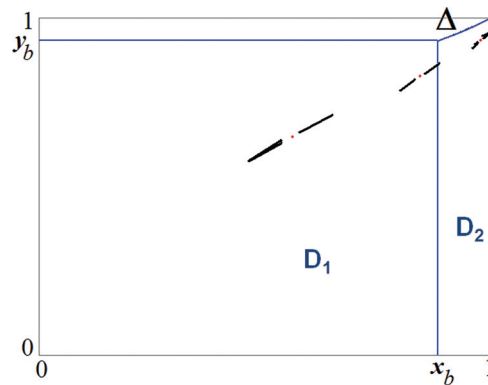


FIG. 8. (Color online) A six-piece chaotic attractor at $\alpha = 1.1$, $\mu = 1.5$, and $\delta = 0.47$.

route: $2k$ -cyclical chaotic sets, then k -cyclical chaotic sets and a chaotic set in one piece, at the homoclinic bifurcation values determined in Proposition 5.

Also fixing a value of α and increasing the parameter δ , a finite number of periodicity regions may be crossed. A route to chaos associated with the 2-cycle at fixed value of α and increasing the parameter δ is illustrated in Fig. 7. Figure 7(a) shows the degenerate flip bifurcation of the 2-cycle, which is followed by the transition to four-piece, two-piece, and one-piece chaotic attractors for the map T .

The occurrences of a six-piece chaotic attractor following the degenerate flip bifurcation of the stable 3-cycle is shown in Fig. 8.

Now we prove that, due to the linearity of the function T_1 , we can also explicitly determine the coordinates of the maximal k -cycles, for any $k \geq 3$, appearing in pairs via border collision bifurcation (at the bifurcation BCB_k given in Proposition 5), one of which may be locally stable while one is necessarily unstable. It is clear that the x -coordinates can be obtained via the equations given in Appendix A and converting them to the original coordinates, by using the inverse function given in Eq. (26). Then, we have to find the y -coordinates of the k -cycles, which depend on the function $T^k(x_n, y_n)$. In order to find one periodic point of such cycles, we consider the one that is closest to the switching value

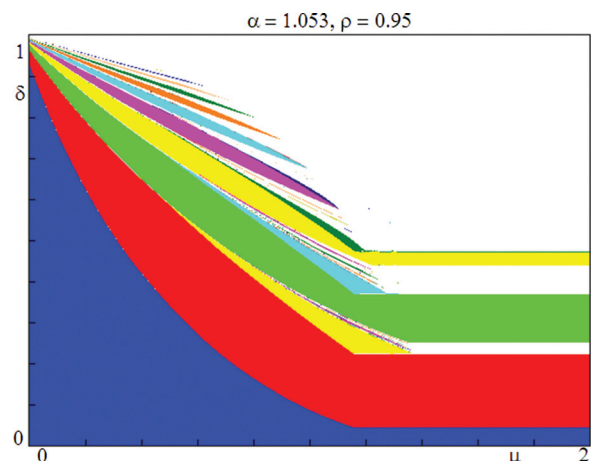


FIG. 9. (Color online) Bifurcation structure for the general model (9) in the parameter plane (μ, δ) , at $\alpha = 1.053$ and $\rho = 0.95$ fixed.

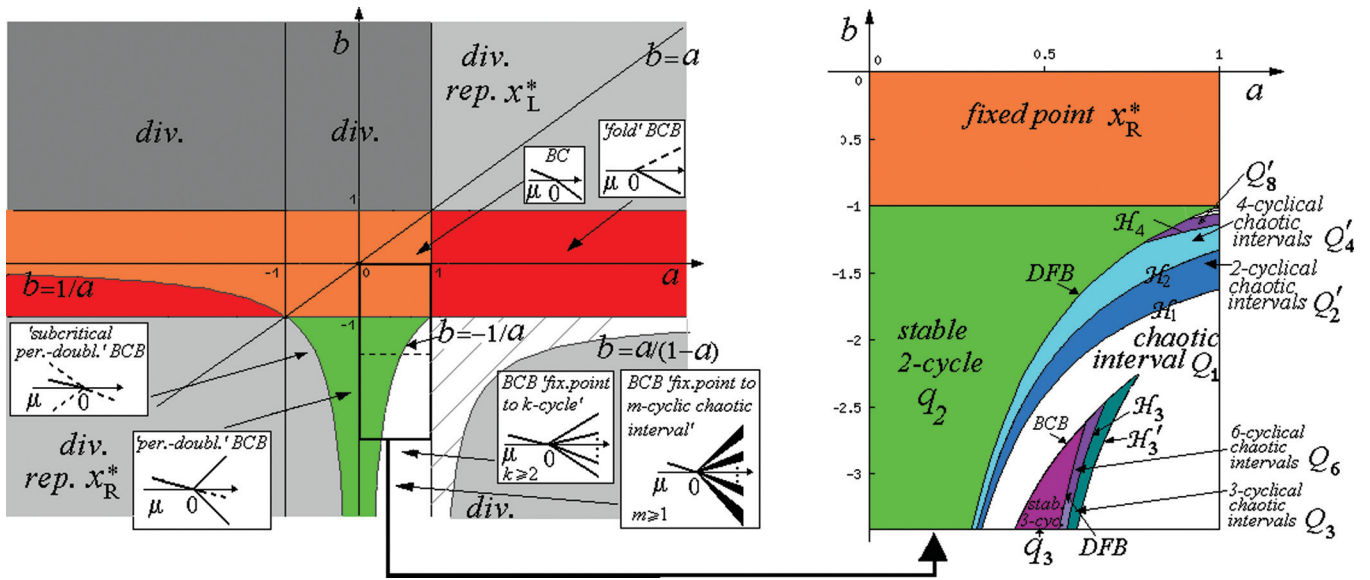


FIG. 10. (Color online) Two-dimensional bifurcation diagram of the skew-tent map given in Eq. (43).

$x = x_b$ on the right side (in the region D_2). So, let us denote by $(x_1^{k,s}, y_1^{k,s})$ the periodic point of the k -cycle, which may be stable, then it is obtained by solving the following equation:

$$T_1^{k-1} \circ T_2(x_1^{k,s}, y_1^{k,s}) = (x_1^{k,s}, y_1^{k,s}). \tag{36}$$

While denoting by $(x_1^{k,u}, y_1^{k,u})$, the periodic point of the k -cycle is always unstable, then it is obtained by solving the following equation:

$$T_1^{k-2} \circ T_2^2(x_1^{k,u}, y_1^{k,u}) = (x_1^{k,u}, y_1^{k,u}). \tag{37}$$

By simple computations we have, for any $n \geq 1$,

$$T_1^n(x, y) = \begin{cases} \delta^n x + \alpha(1 - \delta^n) \\ \delta^{n/\mu} y + \alpha(1 - \delta^{n/\mu}) \end{cases} \tag{38}$$

and the composite functions of T^k that we need are explicitly given as follows:

$$T_1^{k-1} \circ T_2(x, y) = \begin{cases} -\frac{\delta^k}{(\alpha - 1)} x + \frac{\alpha \delta^k}{(\alpha - 1)} + \alpha(1 - \delta^{k-1}) \\ \alpha \delta^{k/\mu} \left(\left(\frac{\alpha - x}{\alpha - 1} \right)^{1/\mu} - 1 \right) + \delta^{k/\mu} y + \alpha(1 - \delta^{(k-1)/\mu}) \end{cases}, \tag{39}$$

$$T_1^{k-2} \circ T_2^2(x, y) = \begin{cases} \frac{\delta^k}{(\alpha - 1)^2} x - \frac{\alpha \delta^k}{(\alpha - 1)^2} + \frac{\alpha \delta^{k-1}}{(\alpha - 1)} + \alpha(1 - \delta^{k-2}) \\ \alpha \delta^{(k-1)/\mu} \left(\left(\frac{\alpha(\alpha - 1) - \delta(\alpha - x)}{(\alpha - 1)^2} \right)^{1/\mu} - 1 \right) + \alpha \delta^{k/\mu} \left(\left(\frac{\alpha - x}{\alpha - 1} \right)^{1/\mu} - 1 \right) + \delta^{k/\mu} y - \alpha \delta^{(k-1)/\mu} \end{cases}. \tag{40}$$

So, by using the expressions in Eqs. (39) and (40), we have the following:

Proposition 6: Let $\mu > 1$ and $1 < \alpha < \alpha^* = 1 + \delta$. Then for any $k \geq 3$, the coordinates of the k -cycles appearing via border collision bifurcation crossing the bifurcation curve BCB_k are given by

$$x_1^{k,s} = \frac{\alpha(\alpha - 1)(1 - \delta^{k-1}) + \alpha \delta^k}{\alpha - 1 + \delta^k}, \quad y_1^{k,s} = \frac{-\alpha \delta^{k/\mu} \left(\left(\frac{\alpha - x_1^{k,s}}{\alpha - 1} \right)^{1/\mu} - 1 \right) + \alpha(1 - \delta^{(k-1)/\mu})}{1 - \delta^{k/\mu}}, \tag{41}$$

$$x_1^{k,u} = \frac{\alpha(\alpha - 1)\delta^{k-1} + \alpha(\alpha - 1)^2(1 - \delta^{k-2}) - \alpha \delta^k}{(\alpha - 1)^2 - \delta^k},$$

$$y_1^{k,u} = \frac{\alpha \delta^{(k-1)/\mu} \left(\left(\frac{\alpha(\alpha - 1) - \delta(\alpha - x_1^{k,u})}{(\alpha - 1)^2} \right)^{1/\mu} - 1 \right) + \alpha \delta^{k/\mu} \left(\left(\frac{\alpha - x_1^{k,u}}{\alpha - 1} \right)^{1/\mu} - 1 \right) + \alpha(1 - \delta^{(k-2)/\mu})}{1 - \delta^{k/\mu}}. \tag{42}$$

V. CONCLUSIONS

In this work, we have considered the bifurcations occurring in a two-dimensional piecewise smooth map describing a circuit proposed in Sec. II as chaos generator. The original results are given in Secs. III and IV, where we have shown how the system is topologically conjugate to one having a particular triangular structure, whose dynamics (characterizing one of the state variables) are strictly related with the piecewise smooth one-dimensional skew-tent map. This particular structure of the model leads to the analytical description of the bifurcation curves, which correspond to border collision bifurcations and to homoclinic bifurcations involving maximal cycles. A peculiarity of the piecewise smooth map is the occurrence of only degenerate flip bifurcations and the direct transition to a robust chaotic regime, which can change in structure only via the cyclic chaotic components. These transitions are due to homoclinic bifurcations, which are also analytically determined. The system here investigated is only a particular case of the circuit described in Sec. II, and we have seen that the dynamics lead to robust chaos. Together with the other particular case, considered in Ref. 28, we are confident that these results are of some help in the analysis of the general case, i.e., of map M defined in Sec. II, in which the parameter ρ is not fixed (here taken equal to 1). In the general model, we obtain more complicated bifurcation structures, as shown in Fig. 9 at $\rho = 0.95$. However, a similarity exists with the phase space of the particular model considered in this work. We leave the analysis of the bifurcations of the general circuit for further studies, for which the present work may be of some help.

ACKNOWLEDGMENTS

This work was supported by the French project ANR05-RNRT02001 ACSCOM (Apport du Chaos dans la Sécurité des systèmes Communicants Optiques et Mobiles).

APPENDIX A: SKEW-TENT MAP

In this appendix, we recall the bifurcations curves of the 1D piecewise linear map f given by two linear functions and defined as

$$f : x \mapsto f(x) = \begin{cases} f_L(x) = ax + 1, & x \leq 0, \\ f_R(x) = bx + 1, & x \geq 0, \end{cases} \quad (A1)$$

where a, b are real parameters with $0 < a < 1$ and $b < 0$, the so-called skew-tent map, because we are interested in these values via the parameters of our map as given in Eq. (11):

$$a = \delta \in (0, 1), \quad b = -\frac{\delta}{\alpha - 1} < 0.$$

The case here considered, increasing/decreasing with maximum in 1, is topologically conjugate to the case decreasing/increasing with minimum in -1 as considered for example in Ref. 32, from which we recall here some results

[to be used in our map in Eq. (11)], noticing that the rich dynamics in this range have already been studied by many authors (see, e.g., Refs. 33, 34, 15, 14, and 35).

The critical point $x = 0$ is the point of maximum, and the absorbing interval I is given by $I = [f^2(0), f(0)] = [b + 1, 1]$. For $a < 1$, f has a unique fixed point $x_R^* = 1/(1 - b) > 0$, which is globally attracting for $b > -1$ and repelling for $b < -1$. The degenerate flip bifurcation of x_R^* at $b = -1$ leads to an attracting 2-cycle having one periodic point in $x < 0$ and one in $x > 0$.

In Fig. 10, it is shown the two-dimensional bifurcation diagram of the (a, b) -parameter plane in the interesting region.

When the fixed point x_R^* is unstable, the map f can have an attracting cycle q_k of any period $k \geq 2$, as well as cyclical chaotic intervals Q_k of any period $k \geq 1$. Let us first describe the routes associated with the cycles of period $k \geq 3$. We shall describe below the effects of the degenerate flip bifurcation of the 2-cycle.

The cycles having period $k \geq 3$ (also called *principal cycles* or *maximal cycles*) appear in pairs, one stable q_k (with the symbolic sequence RL^{k-1}) and one unstable q'_k (with the symbolic sequence R^2L^{k-2}). In Fig. 10, we can see that the curve BCB_3 corresponds to the ‘‘saddle-node’’ BCB, which gives rise to the attracting cycle q_3 and the repelling cycle q'_3 . The right boundary of the stability region $\Pi(q_k)$ of q_3 is the curve DFB_3 corresponding to the degenerate flip bifurcation of the attracting cycle q_3 , which becomes repelling, leading to cyclical chaotic intervals of double period, Q_6 . All these cycles of period $k \geq 3$ undergo the same bifurcation sequence (increasing a), that is, the degenerate flip bifurcation $q_k \Rightarrow Q_{2k}$ is followed by the transitions of cyclical chaotic intervals $Q_{2k} \Rightarrow Q_k \Rightarrow Q_1$. The boundary between the region Q_{2k} and the region Q_k is the curve H_k corresponding to the first homoclinic bifurcation of the cycle q_k , while the right boundary of the region Q_k is the curve H'_k related to the first homoclinic bifurcation of the cycle q'_k , leading to a one-piece chaotic interval $Q_1 = I = [b + 1, 1]$. In the portion of the parameter plane shown in Fig. 10, only the stability region of the cycle q_3 is observable, but in the strip $a \in (0, 0.5)$, all the regions $\Pi(q_k)$ exist where $k \rightarrow \infty$ as b tends to $-\infty$. The bifurcation curves can be detected analytically using the coordinates of the points of the cycles.

In order to find the periodic points of such cycles, we consider the periodic point that is closest to zero on the right side. So, the periodic point $x_1^{k,s}$ of the cycle q_k is obtained by solving the following equation: $f_L^{k-1} \circ f_R(x_1^{k,s}) = x_1^{k,s}$, which leads to the point

$$x_1^{k,s} = \frac{1 - a^k}{(1 - a)(1 - ba^{k-1})}, \quad (A2)$$

while the periodic point $x_1^{k,u}$ of the cycle q'_k is obtained by solving the following equation: $f_L^{k-2} \circ f_R^2(x_1^{k,u}) = x_1^{k,u}$, which leads to the point

$$x_1^{k,u} = \frac{ba^{k-2}(1 - a) + 1 - a^{k-1}}{(1 - a)(1 - b^2a^{k-2})}, \quad (A3)$$

and the BCB occurs when the periodic point $x_1^{k,u}$ collides with the border, $x_1^{k,u} = 0$, that is, for

$$\text{BCB}_k: b = -\frac{1 - a^{k-1}}{(1 - a)a^{k-2}}. \tag{A4}$$

Thus, crossing the BCB curve denoted BCB_k , a pair of cycles appears, a repelling one, q'_k [a periodic point of which is given in Eq. (A3)] and a cycle q_k [a periodic point of which is given in Eq. (A2)], which is attracting for $b < b_k$, where b_k is defined below, while both cycles are repelling if $b > b_k$. The eigenvalue of the stable cycle q_k is given by $\lambda = ba^{k-1}$ so that it loses stability via degenerate flip bifurcation when

$$\text{DFB}_k: b = -\frac{1}{a^{k-1}}. \tag{A5}$$

Thus, the stability region of the cycle q_k is given by $(a, b) \in \Pi(q_k)$, where

$$\Pi(q_k) = \left\{ (a, b) : -\frac{1}{a^{k-1}} \leq b \leq -\frac{1 - a^{k-1}}{(1 - a)a^{k-2}} \right\}, \tag{A6}$$

and it is bounded by the two bifurcation curves BCB_k and DFB_k given in Eqs. (A4) and (A5), which intersect at the point (a_k, b_k) , where a_k is the root of the equation $a^k - 2a + 1 = 0$ in the interval $(0.5, 1)$ and $b_k = -1/a_k^{k-1}$.

The degenerate flip bifurcation of q_k for $k \geq 3$ leads to cyclical chaotic intervals of double period $2k$, denoted by Q_{2k} . The boundaries of the chaotic interval are always given by the point $x = 1$ and its iterates. The attracting $2k$ -cyclical chaotic intervals Q_{2k} exist in the parameter region bounded by the curves BCB_k and DFB_k [given in Eqs. (A4) and (A5), respectively] and by the curve denoted H_k related to the first homoclinic bifurcation of the cycle q_k , given by

$$H_k: a^{2(k-1)}b^3 - b + a = 0. \tag{A7}$$

The transition $Q_{2k} \Rightarrow Q_k$ takes place crossing the curve H_k , while the transition $Q_k \Rightarrow Q_1$ occurs crossing the curve denoted H'_k corresponding to the first homoclinic bifurcation of the cycle q'_k , given by

$$H'_k: a^{k-1}b^2 + b - a = 0. \tag{A8}$$

Now let us consider the 2-cycle. It is possible to see in Fig. 10 that the DFB of the 2-cycle q_2 is particular. The 2-cycle is in fact a particular one because it does not appear by border collision bifurcation (in pair with a repelling one) as it occurs for the other k -cycles. Instead, the 2-cycle appears after the degenerate flip bifurcation of the fixed point x_R^* occurring at $b = -1$. With the equation given in (A2) for $k = 2$, we get the right coordinate of the 2-cycle q_2 , which is without a companion repelling 2-cycle. We have

$$x_R^2 = \frac{1 + a}{1 - ab}, \quad x_L^2 = \frac{1 + b}{1 - ab}, \tag{A9}$$

and its degenerate flip bifurcation occurs when $ab = -1$, thus giving the bifurcation curve shown in Fig. 10. Differently from the cycles q_k for $k \geq 3$ described above, the DFB of q_2 may lead to m -cyclical chaotic intervals of any even period m . That is, we can have the transition $q_2 \Rightarrow Q'_{2m}$, where $m \geq 2$, moreover,

$m \rightarrow \infty$ as $b \rightarrow -1$ and $a = -1/b \rightarrow 1$. Two contiguous regions Q'_{2^i} and $Q'_{2^{i+1}}$ are separated by the curve corresponding to the first homoclinic bifurcation of the 2^i -cycle given by

$$H_{2^i}: b^{\delta_{i+1}} a^{\delta_i} + (-1)^i (b - a) = 0, \tag{A10}$$

where $\delta_m, m = 0, 1, \dots$, are the solutions of the difference equations $\delta_{i+1} = 2\delta_i + (1 + (-1)^i)/2, i = 1, 2, \dots$, with $\delta_0 = 1$ (see Ref. 15 for further details). The bifurcation curve H_1 corresponds to the homoclinic bifurcation of the fixed point x_R^* occurring when $f^3(0) = x_R^*$, that is,

$$H_1: ab^2 + b - a = 0. \tag{A11}$$

APPENDIX B: TRIANGULAR MAP

A dynamical system of the form

$$\mathcal{T}: \begin{cases} x_{n+1} = F(x_n) \\ y_{n+1} = G(x_n, y_n) \end{cases}, \tag{B1}$$

where $F(x_n)$ gives an autonomous state variable, whose dynamics is independent of the values of the other variable, while $G(x_n, y_n)$ depends on both state variables, is called map in triangular form. Here we recall a property that holds for any triangular map:

Property 1: Let $\mathcal{T}(x, y)$ be a triangular map with autonomous variable $x' = F(x)$.

- (1) *If $\{(x_i, y_i)\}_{i=1, \dots, k}$ is a k -cycle of \mathcal{T} , then $\{x_i\}_{i=1, \dots, k}$ is a k -cycle of $F(x)$.*
- (2) *If $\{x_i\}_{i=1, \dots, k}$ is a k -cycle of $F(x)$, then the vertical lines $\{x = x_i\}_{i=1, \dots, k}$ give an invariant set of \mathcal{T} .*
- (3) *The Jacobian matrix DT associated with any cycle of \mathcal{T} is a diagonal matrix whose diagonal terms are the real eigenvalues.*
- (4) *The k th iterate is also triangular, of the form $\mathcal{T}^k(x, y) = (F^k(x), \dots)$.*

The proof is immediate, and it states that all the cycles of the two-dimensional map \mathcal{T} are associated with cycles of the one-dimensional map F (while the vice versa is not necessarily true) and the dynamics of a point belonging to the vertical lines associated with the cycles cannot exit from such vertical lines. The eigenvalues are always real, for any cycle. In particular, for a fixed point (x^*, y^*) of \mathcal{T} , the eigenvalues are $\lambda_1 = (d/dx)F(x)|_{x^*}$, $\lambda_2 = (\partial/\partial y)G(x, y)|_{(x^*, y^*)}$. The eigenvector associated with λ_2 is the vertical line through the fixed point while the eigenvector associated with λ_1 is the line through the fixed point with slope $m = (\partial/\partial x)G(x, y)|_{(x^*, y^*)} / (\lambda_1 - \lambda_2)$. \square

¹T. Kiliyas, K. Kelber, A. Mogel, and W. Schwarz, *Int. J. Electron.* **79**, 737 (1995).

²A. S. Elwakil and A. M. Soliman, *Chaos, Solitons Fractals* **8**, 1921 (1997).

³A. S. Elwakil, K. N. Salama, and M. P. Kennedy, *Int. J. Bifurcation Chaos Appl. Sci. Eng.* **12**, 2885 (2002).

⁴M. Delgado-Restituto and A. Rodríguez-Vázquez, *Proc. IEEE* **90**, 747 (2002).

⁵J. Lu, T. Zhou, G. Chen, and X. Yang, *Chaos* **12**, 1054 (2002).

⁶E. Ott, C. Grebogi, and J. A. Yorke, *Phys. Rev. Lett.* **64**, 1196 (1990).

⁷*Controlling Chaos and Bifurcations in Engineering Systems*, edited by G. Chen (CRC, Boca Raton, FL, 2000).

- ⁸J. Lu and Y. Xi, *Chaos, Solitons Fractals* **17**, 127 (2003).
- ⁹S. Banerjee, J. A. Yorke, and C. Grebogi, *Phys. Rev. Lett.* **80**, 3049 (1998).
- ¹⁰*Nonlinear Phenomena in Power Electronics: Attractors, Bifurcations, Chaos, and Nonlinear Control*, edited by S. Banerjee and G. C. Verghese (IEEE, New York, 2001).
- ¹¹Z. T. Zhusubaliyev and E. Mosekilde, *Bifurcations and Chaos in Piecewise-Smooth Dynamical Systems* (World Scientific, Singapore, 2003).
- ¹²M. di Bernardo, C. J. Budd, A. R. Champneys, and P. Kowalczyk, *Piecewise-Smooth Dynamical Systems: Theory and Applications*, Applied Mathematical Sciences Vol. 163 (Springer, London, 2007).
- ¹³H. E. Nusse and J. A. Yorke, *Physica D* **57**, 39 (1992).
- ¹⁴H. E. Nusse and J. A. Yorke, *Int. J. Bifurcation Chaos Appl. Sci. Eng.* **5**, 189 (1995).
- ¹⁵Y. L. Maistrenko, V. L. Maistrenko, and L. O. Chua, *Int. J. Bifurcation Chaos Appl. Sci. Eng.* **3**, 1557 (1993).
- ¹⁶H. E. Nusse, E. Ott, and J. A. Yorke, *Phys. Rev. E* **49**, 1073 (1994).
- ¹⁷S. Banerjee, M. S. Karthik, G. Yuan, and J. A. Yorke, *IEEE Trans. Circuits Syst., I: Fundam. Theory Appl.* **47**, 389 (2000).
- ¹⁸V. Avrutin, P. S. Dutta, M. Schanz, and S. Banerjee, *Nonlinearity* **23**, 445 (2010).
- ¹⁹L. Gardini, F. Tramontana, and I. Sushko, *Math. Comput. Simul.* **81**, 899 (2010).
- ²⁰S. Banerjee and C. Grebogi, *Phys. Rev. E* **59**, 4052 (1999).
- ²¹M. di Bernardo, M. I. Feigin, S. J. Hogan, and M. E. Homer, *Chaos, Solitons Fractals* **10**, 1881 (1999).
- ²²S. Banerjee, P. Ranjan, and C. Grebogi, *IEEE Trans. Circuits Syst., I: Fundam. Theory Appl.* **47**, 633 (2000).
- ²³Z. T. Zhusubaliyev, E. Mosekilde, S. Maity, S. Mohanan, and S. Banerjee, *Chaos* **16**, 1054 (2006).
- ²⁴I. Sushko and L. Gardini, *Int. J. Bifurcation Chaos Appl. Sci. Eng.* **18**, 1029 (2008).
- ²⁵D. J. W. Simpson and J. D. Meiss, *SIAM J. Appl. Dyn. Syst.* **7**, 795 (2008).
- ²⁶T. Kousaka, Y. Yasuhara, T. Ueta, and H. Kawakami, *Int. J. Bifurcation Chaos Appl. Sci. Eng.* **14**, 3655 (2004).
- ²⁷S. Mandal and S. Banerjee, *National Conference on Nonlinear and Dynamics* (Indian Institute of Technology, Kharagpur, India, 2003).
- ²⁸D. Fournier-Prunaret, P. Chargé, and L. Gardini, *Commun. Nonlinear Sci. Numer. Simul.* **16**, 916 (2011).
- ²⁹S. F. Kolyada, *Ergod. Theory Dyn. Syst.* **12**, 749 (1992).
- ³⁰S. F. Kolyada and L. Snoha, in *Iteration Theory*, edited by W. Forg-Rob, D. Gronaw, C. Mira, N. Netzer, and C. Targonsky (World Scientific, Singapore, 1996), p. 165.
- ³¹V. Jeménez and J. Smital, *Fundam. Math.* **167**, 1 (2001).
- ³²I. Sushko and L. Gardini, *Int. J. Bifurcation Chaos Appl. Sci. Eng.* **20**, 2045 (2010).
- ³³S. Ito, S. Tanaka, and H. Nakada, *Tokyo J. Math.* **2**, 241 (1979).
- ³⁴F. Takens, "Dynamical systems and bifurcation theory," in *Research Notes in Mathematics Series, 160*, edited by M. I. Camacho, M. J. Pacifico, and F. Takens (Longman Scientific and Technical, Pitman, 1987), p. 399.
- ³⁵S. Banerjee, M. S. Karthik, G. Yuan, and J. A. Yorke, *IEEE Trans. Circuits Syst., I: Fundam. Theory Appl.* **47**, 389 (2000).
- ³⁶This kind of bifurcation is typical in piecewise linear and hyperbolic systems, as shown in Ref. 32, and to our knowledge it is the first example in a two-dimensional piecewise smooth system not linear-fractional.
- ³⁷In the conjugated case, for $0 < \mu < 1$ the regions involved are D_1 and D_3 , the functions involved are T_1 and T_3 , and now it is the value of y_{n+1} which depends only on y_n .
- ³⁸We recall the definition. A k -cycle of a piecewise smooth map $T(X)$ (of a space $X \subset \mathbb{R}^n$ into itself) undergoes a degenerate flip bifurcation when no point of the cycle coincides with any of the break points, an eigenvalue λ crosses -1 at a bifurcation value in which the k th iterate of the map T^k has locally (in a neighborhood of the related fixed points) infinitely many 2-cycles, that is, locally (in suitable sets) the map satisfies $T^{2k}(X) = X$.